

# SATELLITE IMAGES IN ENVIRONMENTAL DATA PROCESSING

Magdaléna Kolínová Aleš Procházka Martin Slavík

*Prague Institute of Chemical Technology  
Department of Computing and Control Engineering  
Technická 1905, 166 28 Prague 6, Czech Republic  
E-mail: Magdalena.Kolinova@vscht.cz*

**Abstract:** The paper presented deals with various types of satellite data. It discusses methods of satellite data obtaining, of common coordinates used and problems which need to be solved in order to transform the satellite images from one coordinate system to another, to allow for their further processing in respect of environmental data concerning air pollution, including application of de-noising and filtering methods. Besides of an interesting overview of the satellite data issues, their use in environmental data processing is discussed together with the utilization of geographical information systems in the area concerned.

**Keywords:** Image processing, signal de-noising, detection, image enhancement, environmental engineering, geographical information systems

## 1. INTRODUCTION

The paper discusses problems of image analysis and processing (Chellapa, 1992; Watkins et al., 1993; Klette and Zamperoni, 1994; Van der Heijden, 1994) applied to satellite images (Lenoble and Brogniez, 1984; Kaufman and Tanré, 1994) allowing to observe air pollution caused by the dust particles concentration. Fig. 1 presents results of data observation obtained by MODIS (Moderate-Resolution Imaging Spectroradiometer) used for complex research (Kaufman and Tanré, 2004) of the Earth forming a part of the so-called Earth Observing System (EOS) operated by National Aeronautics and Space Administration (NASA).

Satellite observations can be then correlated with the corresponding data of concentration of solid particles obtained by about 100 ground measuring stations precisely defined by their longitude and latitude. Interpolation to the whole area of Czech republic has been applied in this case to obtain the same resolution as that of satellite observations.

The efficient use of correlation methods assumes in many cases proper signal preprocessing to remove specific signal components and to reduce substantial signal errors.

## 2. REMOTE SATELLITE SENSING

At present there are many satellites that are orbiting the Earth and providing new information gathered all around the globe. Their instruments are also able to detect air pollution above the land.

One kind of satellite sensors is operated by NOAA (The National Oceanic and Atmospheric Administration). All these satellites fly on elliptical or circular orbits around the planet earth, the earth's centre being the focal or central point and they belong to the so-called polar orbiting satellites



Fig. 1. A satellite image of the Czech Republic from the Moderate-Resolution Imaging Spectroradiometer - MODIS

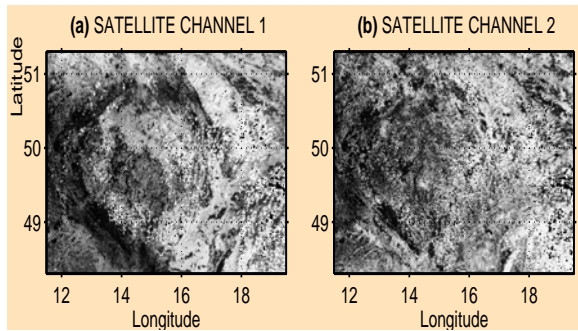


Fig. 2. Satellite image of the Czech Republic from the NOAA satellite at two different channels

which fly in rather low altitudes, typically at 850 km height. Each full orbit around the earth takes 100 minutes, 14 orbits are achieved per day. These orbits are usually sun-synchronous, i.e. the satellite crosses a certain point always at the same time of the day. Polar orbiters provide excellent pictures of all parts of the earth including the polar regions. Due to their orbital characteristics they cannot monitor short-term variations. The main apparatus of NOAA satellites is the scanning radiometer AVHRR (Advanced Very High Resolution Radiometer). This is a five-channel apparatus covering spectral ranges (1)  $0.58\text{-}0.68\mu\text{m}$ , (2)  $0.725\text{-}1.1\mu\text{m}$ , (3)  $3.55\text{-}3.93\mu\text{m}$ , (4)  $10.3\text{-}11.3\mu\text{m}$ , (5)  $11.5\text{-}12.5\mu\text{m}$ . The first two channels work with the reflected sun radiation only in red and close infrared region, the last two ones are fully heat radiation channels, and channel 3 is a mixed one. An example of the NOAA observation of Czech Republic is in Fig. 2.

A sample observation of the Czech Republic in a selected time is presented in Fig. 2 for the first and the second channel taken by the NOAA satellite. Different channels observe the ground at different frequency lengths. It is assumed that images obtained contain the same information about surface objects, and they differ in reflection of presence of aerosol particles, and they differ in reflection of presence of aerosol particles. Correlation between these two images can thus be used for detection of aerosol particles, localization of sources of their immission and possible prediction of this type of air pollution.

Another type of satellites, represented by Meteosat satellites have a geostationary orbit having at the height of 36000 km above the equator the orbital period exactly equal to 24 hours and thus equal to the orbital period of the earth itself. The satellite is therefore above the same point of the earth's surface and it always views the same portion of the globe. Due to its position above the equator a geostationary satellite only gives a very distorted view of the polar regions where they is of practically no use. With the exception of these high latitudes the existing system of geostationary meteorological satellites gives a global view of our planet.

Further sensor is the Moderate-Resolution Imaging Spectroradiometer (MODIS) that gathers information and properties of the land, the oceans and the atmosphere. At present two MODIS instruments (Kaufman and Tanré, 2004) are on the Earth's orbit on board of two platforms Terra and Aqua (officially known as EOS AM-1 and EOS PM-1 respectively). These two satellites are on sun synchronous near-polar orbit with period of 99 minutes in the altitude of 705 km. The term "near-polar" points to fact that the satellites are mowing in north-south direction. The term "sun synchronous" points to fact that the satellite is above any parallel at a same local time. In other words the angle between satellite, the Earth's surface below the satellite and the Sun is always the same.

The orbit of the satellites is very important because of at least two reasons. The first reason is that MODIS and other on board sensors are detecting solar radiation reflected from the Earth's surface and atmosphere. The second reason is that these sensors are scanning the whole surface of the Earth every one or two days.

The MODIS instrument is intended to measure reflected sun radiation using highly sensitive detectors in 36 spectral bands that range in wavelength from  $0.4\ \mu\text{m}$  to  $14.4\ \mu\text{m}$  with resolution from 250 m to 1 km. This provides an unprecedented look at terrestrial, atmospheric, and ocean phenomenology. Fig. 3 illustrates the difference to have comparison of MODIS resolution abilities.



Fig. 3. Comparison of the image obtained by the Advanced Very High Resolution Radiometer-AVHRR (on the left) and by MODIS (on the right)

### 3. IMAGE PROCESSING

#### 3.1 Image De-noising

Digital filtering techniques allow both linear and non-linear image processing. They can be used efficiently to remove various forms of noise from the processed data or some other specific parts of the data the presence of which is not desirable in further processing. In all these cases, the convolution kernel  $\mathbf{H}_{K,J}$  of the filter applied moves

along all rows and columns of the image data  $\mathbf{A}_{M,N}$ , modifying values of individual points of the image according to conditions specified by the two dimensional convolution

$$B(m+K/2, n+J/2) = \sum_{k=1}^K \sum_{j=1}^J H(k, j) A(m-k, n-j)$$

In the most simple case, the mean value of a certain subimage matrix moving through the whole image is computed for every point of the image using the same values of the convolution kernel evaluated as a reciprocal value of the number of kernel values.

Application of more sophisticated FIR filters makes it possible to evaluate values of a convolution kernel in a more precise way to reject selected image spectral components. Assuming the desired frequency response

$$|\text{Dft}\{H(k, j)\}| = \begin{cases} e^{-j\omega_1\alpha_1} e^{-j\omega_2\alpha_2} & \text{for } -\omega_{1c} < \omega_1 < \omega_{1c} \\ & -\omega_{2c} < \omega_2 < \omega_{2c} \\ 0 & \text{elsewhere} \end{cases}$$

we obtain the filter coefficients by applying the formula for the two dimensional Fourier series, and we find the following solution for the coefficients

$$H(k, j) = \frac{\sin \omega_{1c}(k - \alpha_1)}{k - \alpha_1} \frac{\sin \omega_{2c}(j - \alpha_2)}{j - \alpha_2} \quad (1)$$

where  $\alpha_1 = \frac{K-1}{2}$  and  $\alpha_2 = \frac{L-1}{2}$ .

Fig. 4 presents a simulated two dimensional signal which is shown with added noise, its spectrum together with frequency characteristics of FIR filter and then the same image de-noised using the designed FIR filter. A similar method has been used for satellite data processing for evaluation of the air pollution (Kolínová and Procházka, 1999).

Median filtering (Chellapa and Sawchuk, 1985; Tukey, 1971) standing for a non-linear method allows a very efficient removal of singularities in an observed sequence or image. This method is very often applied especially in image processing assuming application of overlapping matrices of size limited to 3 by 3 only. The central element of this matrix moves along all rows and columns

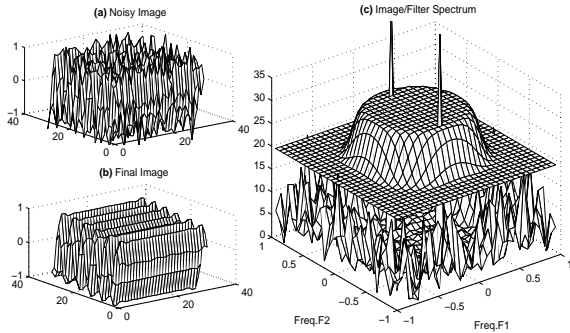


Fig. 4. Image de-noising presenting (a) a simulated image (b) its spectrum together with the spectrum of the convolution kernel and (c) the final de-noised image

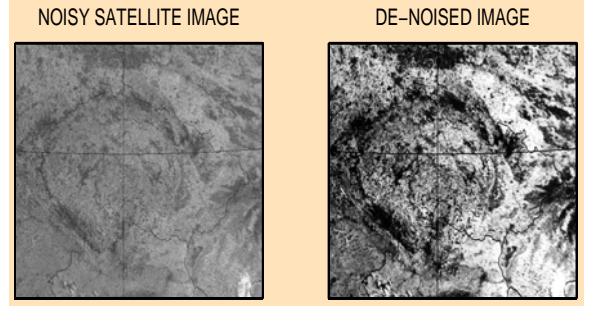


Fig. 5. An example of satellite image de-noising of the original image. The median value of the given subimage belonging to this window is then used instead of its reference element in every case. This method has been applied to remove specific elements of satellite images, especially the meridian that forms a part of original data. An example of real data de-noising is given in Fig. 5.

Image de-noising has been studied also in connection with image decomposition and reconstruction by wavelet transforms (N.G. Kingsbury and J.F.A. Mugarey, 1998). This method provides a very efficient tool for image de-noising as well.

### 3.2 Image Correlation

Correlation of two images stored in two matrices assumes evaluation of the correlation coefficient for the corresponding subimage regions in matrices  $\mathbf{A}$  and  $\mathbf{B}$  which can be obtained using the relation

$$r = \frac{\sum_m \sum_n (A(m, n) - \bar{A})(B(m, n) - \bar{B})}{\sqrt{\sum_m \sum_n (A(m, n) - \bar{A})^2 \sum_m \sum_n (B(m, n) - \bar{B})^2}} \quad (2)$$

where  $\bar{A}$  and  $\bar{B}$  represent the mean values of the respective matrices  $\mathbf{A}$  and  $\mathbf{B}$ .

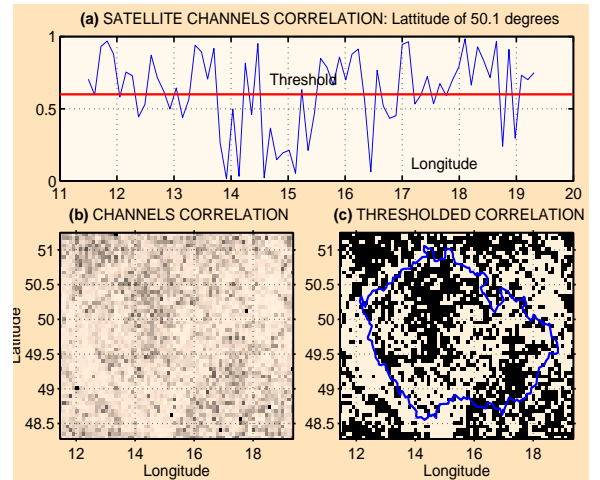


Fig. 6. Thresholded correlation function of images of the Czech Republic from the NOAA satellite



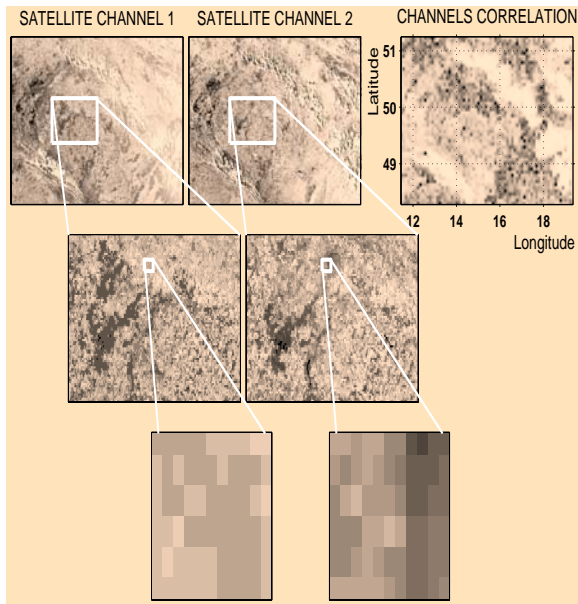


Fig. 7. Thresholded correlation function of images of the Czech Republic from the NOAA satellite

Results of this correlation for images covering the area of 10 by 10 pixels corresponding to the region of 0.1 by 0.05 degrees in longitude and latitude, respectively, are presented in Fig. 6. As the low coefficient can be used as a measure for aerosol particles, Fig. 6 presents the distribution of this variable below a certain threshold level only.

#### 4. RESULTS

The process of estimation of air pollution obtained from two channels of satellite observations based on their correlation is presented in Fig. 7 at a chosen time instant. Comparison of these results for several different pairs of observations is presented in Fig. 8 pointing to regions with the highest air pollution for a specific threshold limit.

Further research devoted to comparison of results obtained from satellite observations with that obtained from ground measuring stations proved correlation between these two kinds of air pollution estimations.

Owing to verification of the proposed method it has been possible to compare air pollution concentration in urban and rural regions of the Czech Republic.

#### 5. CONCLUSION

Results presented in the paper justify correspondence between satellite and ground observations in the case of appropriate weather conditions as

correlation of the surface and satellite measurements gives very satisfactory results for some regions in which the concentration of aerosol particles in the air is measured.

We can state that the satellite images do indeed contain information on air pollution. More detailed statements on how such information will be used for evaluation of air pollution will be made after greater volumes of data are processed. The precision of data observed must be studied in this connection as well.

Studies of the given data motivate subsequent research of general mathematical problems and they form a basis for further research in this area. It is assumed that these studies will include methods for satellite images de-noising, enhancement and correlation with ground measurements.

A very important topic of further research is in the study of geographical information systems to connect observed images with their geographical locations and to find geographical coordinates of each observed pixel as precisely as possible. Different geographical systems can be used in these studies.

#### ACKNOWLEDGMENTS

The work has been supported by the research grant of the Faculty of Chemical Engineering of the Institute of Chemical Technology, Prague No. MSM 6046137306.

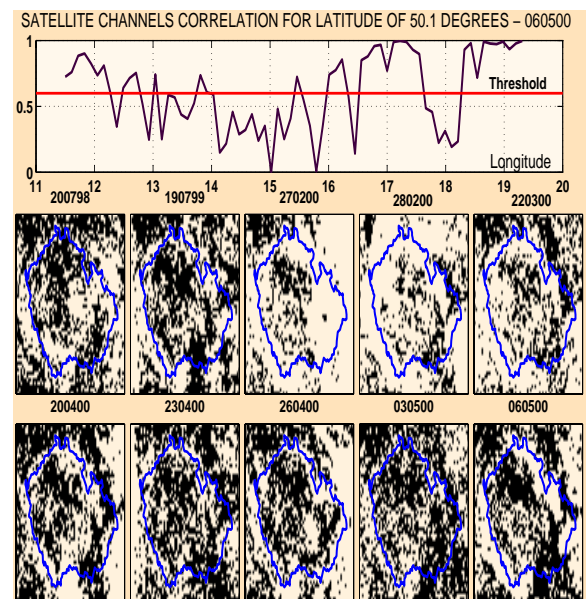


Fig. 8. Thresholded correlation function of images of the Czech Republic from the NOAA satellite

## References

- R. Chellapa. *Digital Image Processing*. IEEE Computer Society Press, Los Alamitos, 1992.
- R. Chellapa and A. A. Sawchuk. *Digital Image Processing and Analysis: Volume 1: Digital Image Processing*. IEEE Computer Society Press, Silver Spring, 1985.
- Y. J. Kaufman and D. Tanré. Variations in cloud supersaturation and the aerosol indirect effect on climate. *Nature*, 369:45–48, 1994.
- Y. J. Kaufman and D. Tanré. Algorithm for remote sensing of tropospheric aerosol from modis. Technical report, [http://modis.gsfc.nasa.gov/data/atbd/atbd\\_mod02.pdf](http://modis.gsfc.nasa.gov/data/atbd/atbd_mod02.pdf), 2004.
- R. Klette and P. Zamperoni. *Handbook of Image Processing Operators*. John Wiley & Sons, New York, 1994.
- M. Kolínová and A. Procházka. Two-Dimensional Fourier Transform in Image Noise Rejection. In *Process Control '99*, Tatranske Matliare, 1999. Slovak University of Technology.
- J. Lenoble and C. Brogniez. A comparative review of radiation aerosol models. *Britr. Phys. Atmosph.*, 57(1):1–20, December 1984.
- N.G. Kingsbury and J.F.A. Mugarey. Wavelet Transforms in Image Processing. In A. Procházka, J. Uhlíř, P. J. W. Rayner, and N. G. Kingsbury, editors, *Signal Analysis and Prediction*, Applied and Numerical Harmonic Analysis, chapter 2. Birkhauser, Boston, U.S.A., 1998.
- J. W. Tukey. *Exploratory Data Analysis (preliminary ed.)*. Addison-Wesley, Reading, 1971.
- F. Van der Heijden. *Image Based Measurement Systems*. John Wiley & Sons, New York, 1994.
- Ch. Watkins, A. Sadun, and S. Marenka. *Modern Image Processing: Warping, Morphing, and Classical Techniques*. Academic Press, Ltd., London, 1993.